



2013 ISES Solar World Congress

## Semi-Passive Solar Tracking Concentrator

Noel León<sup>a</sup>, Héctor García<sup>a</sup>, Carlos Ramírez<sup>a,\*</sup>

<sup>a</sup>*Tecnológico de Monterrey, Eugenio Garza Sada 2501, Monterrey, 64849, México*

### Abstract

A solar tracking concentrator (STC) has to adapt to the changes in the sun's position throughout the day and even more so, throughout the year. The function of sun tracking is to keep the sun's rays perpendicular to the absorber's cross-sectional area through a constant orientation, which requires an accurate electro-mechanical system that increases the cost of the whole concentrator. Sun tracking enables solar radiation to be concentrated in a limited and well-defined area of a receiver where the thermal energy collected is stored and then transformed into other kinds of energy. This heightens the prospects for the STC to use as little energy and movement as possible for solar tracking so as to achieve such a concentration. For this reason, a semi-passive solar tracking concentrator (SPSTC) whose configuration requires a minimal mechanical effort and reduced movement for sun tracking is proposed. It mainly consists of a micro-heliostat array, a Fresnel lens and a receiver. The array tracks the position of the sun to reflect the sun's rays toward the Fresnel lens, which remains horizontal, reducing wind loads over the whole system. The receiver, located on the lens focus, remains stationary, releasing its weight on the sun tracking system and thus reducing the energy required for movement. The SPSTC's kinematics for both altitude and azimuth tracking on a 25°39'15''N latitude is analyzed. An optimum fixed array's tilt of 49.054° was found to maximize the effective Fresnel lens area by reducing blocking and shading, both caused by the position of the array above the lens.

© 2014 The Authors. Published by Elsevier Ltd. This is an open access article under the CC BY-NC-ND license (<http://creativecommons.org/licenses/by-nc-nd/3.0/>).

Selection and/or peer-review under responsibility of ISES.

*Keywords:* Solar tracking system; solar concentrator; Fresnel lens; micro-heliostats

### 1. Introduction

Solar tracking concentrators (STC) are optical systems that focus solar thermal energy on a small area of a receiver. Solar concentration is achieved by exposing to the sun an absorber, whose geometry and optical properties deflect the sun's rays toward a spot or linear focus.

\* Corresponding author. Tel.: +01-52-81-8358-2000.

E-mail address: [A00614747@itesm.mx](mailto:A00614747@itesm.mx)

Nomenclature		Greek symbols	
A	area (m <sup>2</sup> )	$\alpha$	altitude angle (°)
b	blocking (m)	$\beta$	azimuth angle (°)
C	sun's quadrant location	$\beta'$	pseudo-azimuth angle (°)
d	distance between micro-heliostats (m)	$\gamma$	angle between incident ray and micro-heliostat (°)
l	large (m)	$\delta$	angle between reflected ray and micro-heliostat (°)
N	number of micro-heliostats on the array	$\varepsilon$	array's tilt (°)
n	refractive index	$\varphi$	latitude
s	shading (m)		
t	thickness of micro-heliostat (m)		
w	wide (m)		
		Subscripts	
		b	blocking
		e	effective
		F	Fresnel lens
		f	final
		s	shading

The cost of the STC can be reduced by minimizing the need for sun tracking. To achieve this, the following contradiction has to be resolved: on the one hand, the STC has to adapt to the changes in the sun's position to achieve concentration of energy on the receiver. On the other hand, a non-movement STC is desirable in order to simplify its configuration, thus reducing energy consumption and, therefore, the cost. In the literature several STCs have been reported that solve this contradiction by tracking the sun in a passive or semi-passive way. The proposals vary from Fresnel lenses and parabolic mirrors with an unconventional geometry [1-7] to interactions between lenses and mirrors [8-9] and lenses with variable optical properties [10-11]. However, reducing or eliminating sun tracking is still a high-cost solution due to special geometry manufacturing or the need for optical property change equipment. In addition, the sun tracking reduction limits the concentration's efficiency, as several of the sun's rays are deflected before they reach the focus.

In this research, a semi-passive solar tracking concentrator (SPSTC) with reduced sun tracking movement and mechanical effort for minimal solar ray deflection is proposed. It mainly consists of a micro-heliostat array, a spot Fresnel lens and a receiver. Movement for altitude and azimuth sun tracking is calculated in  $\varphi=25^{\circ}39'15''\text{N}$ . An optimal array's tilt is found for Fresnel lens effective area maximization, as this is affected by two factors: blocking and shading, both caused by the position of the array above the lens.

## 2. Semi-passive solar tracking concentrator (SPSTC)

The SPSTC is an optical system that concentrates solar energy with reduced movement and mechanical effort for sun tracking. It mainly consists of a micro-heliostat array, a Fresnel lens and a receiver (see Fig. 1). The micro-heliostat array tracks the sun's position and reflects the sun's rays toward the Fresnel lens, which remains horizontal, thus reducing wind loads over the whole concentrator. Its configuration allows for a stationary receiver, which releases considerable weight in the mechanical sun tracking system. A detailed description of each component is given below.

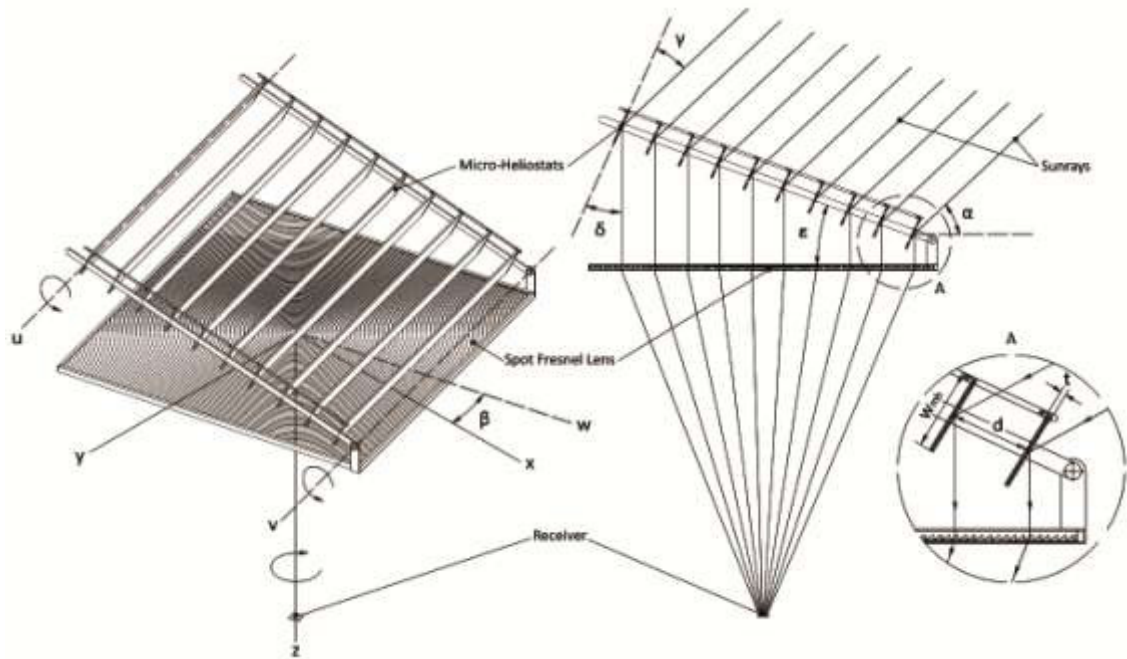


Fig. 1. SPSTC composed of a micro-heliostat array, a Fresnel lens and a receiver

### 2.1 Micro-heliostat array

The micro-heliostats are an array of mirrors located above the Fresnel lens. The array's function is to reflect the sun's rays toward the lens by tracking the sun's path on both angles: altitude and azimuth. The altitude angle is formed between the direction of the incident ray of the sun and its projection on the horizontal plane. The azimuth angle, on the other hand, is formed between this projection and the southern axis. Both angles vary depending on the hour, month and latitude.

Sun tracking for these angles is achieved by the array's rotation around three axes:  $u$ ,  $z$  and  $v$ . The first movement is around the  $u$ -axis, where a synchronized rotation of the micro-heliostats is performed, transforming  $\alpha$  into  $\delta$ , so the direction of the sun's rays remains perpendicular to the cross-sectional area of the the Fresnel lens. To achieve this, the micro-heliostats' rotation follows the reflection law, where the entrance angle  $\gamma$  is equal to the output angle  $\delta$ . The second movement is around the  $v$ -axis, where an angle  $\epsilon$  between the array and the Fresnel lens is formed. This rotation increases the quantity of solar rays reflected by the micro-heliostats by adjusting the array's tilt according to the solar altitude. Finally, the array and lens rotate around the  $z$ -axis to track  $\beta$ , so the array and lens are always aligned to the sun. The three axis rotation varies according to the latitude of installation, in this case, considered as  $25^{\circ}39'15''\text{N}$ .

The values of  $\delta$  for the  $\alpha$ -tracking can be calculated by the following equation:

$$\delta = (90^{\circ} - \alpha) / 2 \quad (1)$$

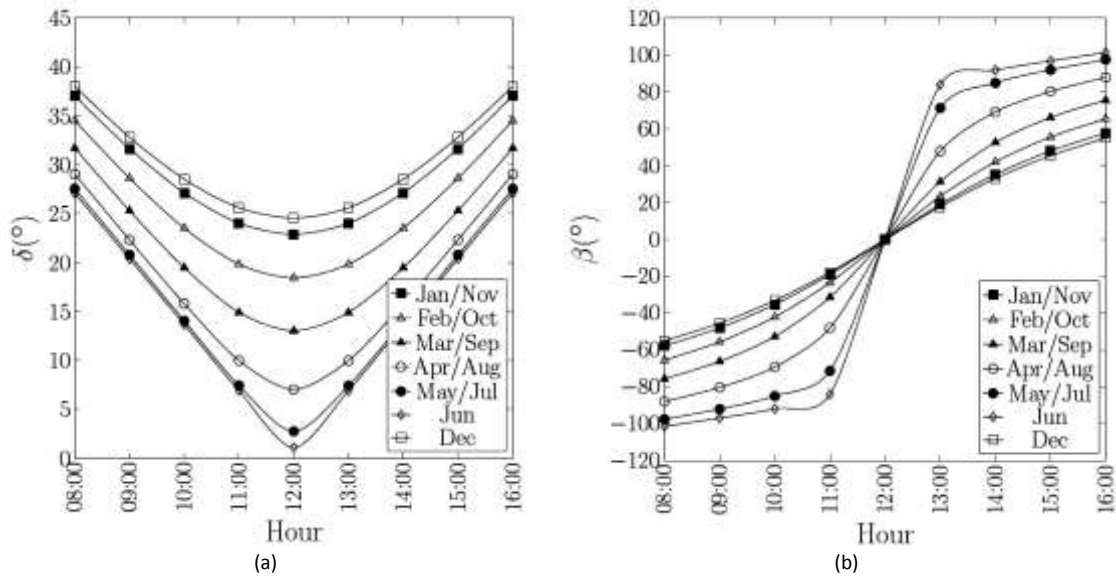


Fig. 2. (a) Micro-heliostats' rotation around  $u$ -axis to track the altitude solar angle  $\alpha$ ; (b) Fresnel lens and array's rotation around  $z$ -axis to track the azimuthal solar angle  $\beta$

The profiles of  $\delta$  are shown in Fig. 2(a). It can be observed that  $\delta$  rotates between  $0^\circ$  and  $40^\circ$  approximately, with different profiles within this range depending on the month of the year. Maximum values occur in the morning and evening and minimum ones, at noon.

On the other hand, the  $\beta$ -tracking can be calculated by an equation for the mathematical model of the sun's movement described in [12]. As this model is beyond the scope of this research, the equation for  $\beta$  is only expressed as follows:

$$\beta = C_1 C_2 \beta' + C_3 \left( \frac{1 - C_1 C_2}{2} \right) 180 \quad (2)$$

The values of  $\beta$  are shown in Fig. 2(b). It can be observed that  $\beta$  rotates between  $-100^\circ$  and  $100^\circ$  approximately. As  $\delta$ , its profile varies according to the month of the year, taking a  $0^\circ$  value at noon. The last type of rotation is around the  $v$ -axis, where the array's tilt varies to adapt to solar path changes throughout the year, reducing blocking and shading, both described in more detail in section 3.

## 2.2 Fresnel lens and receiver

The Fresnel lens is a kind of a solar concentrator that focuses solar radiation on a small area. Its function is to receive the sun's rays reflected by the micro-heliostats and concentrate them on the receiver. This concentration is achieved by two factors. The first one is the refractive index change of the medium where the beam travels, in this case from air ( $n=1.0$ ) to the lens material, typically PMMA ( $n=1.49$ ) and vice versa. The second is caused by the prism array geometry of the lens. More information about the Fresnel lens and the receiver can be found in [13].

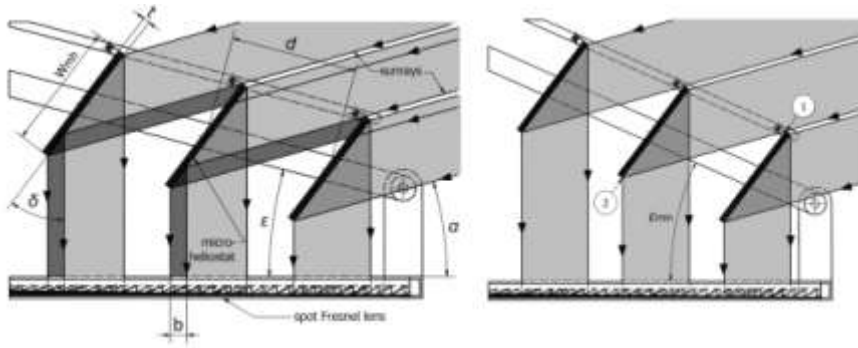


Fig. 3. Blocking caused when the passage of some rays toward a micro-heliostat is interrupted by another micro-heliostat. To avoid it, the array's tilt must be  $\epsilon_{min}$  as a minimum so the beam touches corner 1 of a micro-heliostat and corner 2 of the next micro-heliostat. As it is assumed that all rays reaching the Fresnel lens cross-sectional area at  $90^\circ$  are concentrated on the receiver, only a section of the array and the lens is shown.

### 3. Solar collection area

The solar collection area of a Fresnel lens is equal to its area as long as a shadow is not projected on it. In the SPSTC, the array's position interrupts the passage of some rays toward the lens, reducing its solar collection area by blocking and shading, terms previously used by [14].

#### 3.1 Blocking

Blocking is a factor that reduces the Fresnel lens's useful area and, therefore, the amount of solar energy on the receiver. This is caused by the distance between the micro-heliostats and the array's tilt. There are two types of blocking. The first occurs when the passage of some rays toward a micro-heliostat is interrupted by another micro-heliostat. This takes place when  $\epsilon < \epsilon_{min}$  (see Fig. 3). In the second case, the passage of some rays reflected by a micro-heliostat toward the lens is interrupted by another micro-heliostat. This occurs when  $\epsilon > \epsilon_{max}$  (see Fig. 4). Both types of blocking are expressed by

$$b = \begin{cases} (t \cos \delta + w_{mh} \sin \delta - d \sin(\alpha + \epsilon))(N - 1), & \text{if } \epsilon < \epsilon_{min} \\ (t \cos \delta + w_{mh} \sin \delta - d \cos \epsilon)(N - 1) & \text{if } \epsilon > \epsilon_{max} \\ 0, & \text{if } \epsilon_{min} \leq \epsilon \leq \epsilon_{max} \end{cases} \quad (3)$$

For calculation purposes, the values of  $t=0.005\text{m}$ ,  $w_{mh}=0.1\text{m}$ ,  $d=0.1\text{m}$  and  $N=10$  remain constant. The array's tilt  $\epsilon_{min}$  and  $\epsilon_{max}$  expressed in (3) are obtained by

$$\epsilon_{min} = \left( \frac{\sin \delta (w_{mh} + \tan(\delta + \alpha)t)}{d} \right) \sin^{-1} - \alpha \quad (4)$$

$$\epsilon_{max} = \left( \frac{w_{mh} \sin \delta + t \cos \delta}{d} \right) \cos^{-1} \quad (5)$$

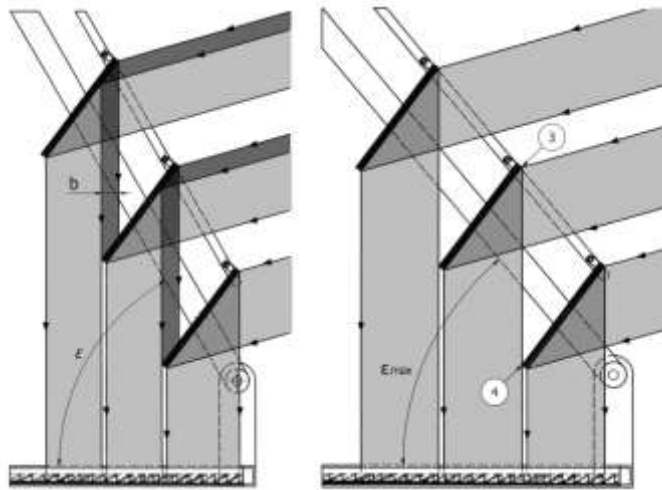


Fig. 4. Blocking caused when the passage of some rays reflected by a micro-heliostat toward the Fresnel lens is interrupted by another micro-heliostat. To avoid it, the array's tilt must be  $\epsilon_{max}$  as a maximum so that the beam touches corner 3 of a micro-heliostat and corner 4 of the previous micro-heliostat.

To avoid blocking, the array must be tilted. To obtain the required tilt, the angle must be between  $\epsilon_{min}$  and  $\epsilon_{max}$ . This range can be calculated by using equations (4) and (5). The variability of this range is shown in Fig. 5. In June, there are more possible values for  $\epsilon$  because the sun's path is almost directly above the system. In December, by contrast, its values are limited because the sun's path is closer to the horizon. Whatever the month, the array's tilt cannot be less than  $0^\circ$  so as to avoid a collision with the lens.

With  $\epsilon_{min}$  and  $\epsilon_{max}$  established, it can be observed that there is a range of between  $26.988^\circ$  and  $49.054^\circ$  where blocking is avoided at any hour and in any month. In other words, the rotation around the  $\nu$ -axis is not required as long as the array's tilt remains constant within this range.

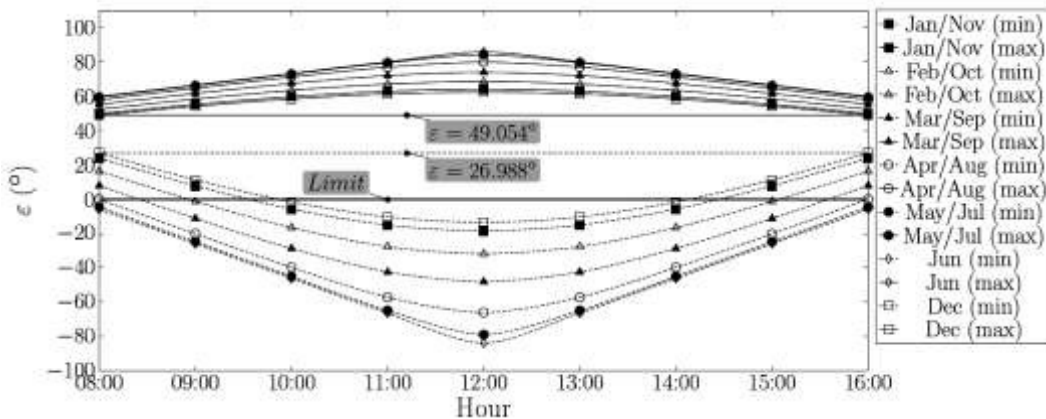


Fig. 5. Values of  $\epsilon$  that avoid blocking. Solid lines represent the maximum values and dotted lines, the minimum ones. The line in  $\epsilon=0^\circ$  represents its lowest limit, as the array's tilt cannot be negative. Any value between  $26.988^\circ$  and  $49.054^\circ$  avoids blocking at any hour and in any month.

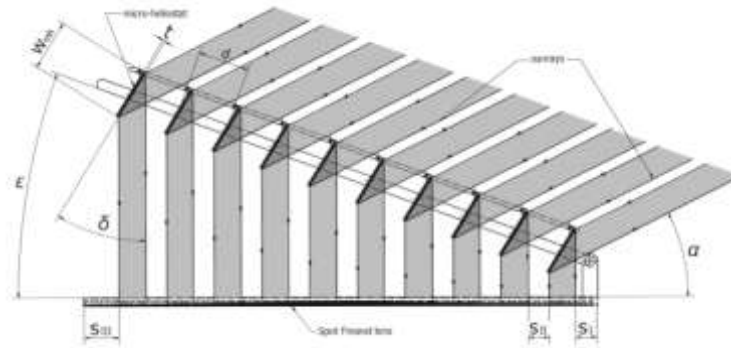


Fig. 6. Types of shading on the Fresnel lens

### 3.2 Shading

The Fresnel lens area is reduced by another factor called shading. Like blocking, it is mainly caused by the distance between the micro-heliostats and the array's tilt. Shading creates Fresnel lens zones where the sun's rays do not impact perpendicular to the cross-sectional area. In the SPSTC, there are three types of shading:  $s_I$ ,  $s_{II}$  and  $s_{III}$  (see Fig. 6).  $s_I$  is formed between the first micro-heliostat and the initial edge of the Fresnel lens;  $s_{II}$  is the projection on the lens mainly formed by the micro-heliostats' distance; and  $s_{III}$  is the shade between the last micro-heliostat and the final edge of the lens. The equations that describe the three types of shading are expressed by

$$s_I = \begin{cases} (d \cos \epsilon - w_{mh} \sin \delta - t \cos \delta) / 2, & \text{if } \epsilon < \epsilon_{\max} \\ 0, & \text{if } \epsilon \geq \epsilon_{\max} \end{cases} \quad (6)$$

$$s_{II} = \begin{cases} (d \cos \epsilon - w_{mh} \sin \delta)(N - 1), & \text{if } \epsilon < \epsilon_{\max} \\ t \cos \delta(N - 1), & \text{if } \epsilon \geq \epsilon_{\max} \end{cases} \quad (7)$$

$$s_{III} = w_F + (t \cos \delta - w_{mh} \sin \delta) / 2 + \cos \epsilon (w_{mh} / 2 - dN) \quad (8)$$

$$s = s_I + s_{II} + s_{III} \quad (9)$$

where  $w_F=1.0\text{m}$ . The ideal case is when the total shading zone in equation (9) is equal to  $0.0\text{m}$ , a value that represents a cross-sectional Fresnel lens area fully covered by perpendicular rays of the sun. The shading area is obtained using

$$A_s = l_{FS} \quad (10)$$

In this case,  $l_F=1.0\text{m}$ . To calculate  $s$  in expression (9), values of  $\epsilon=26.988^\circ$ ,  $38.021^\circ$  and  $49.054^\circ$  were taken into account. So far, the study has been limited to a  $1\text{m}^2$  Fresnel lens with values of  $t$ ,  $w_{mh}$ ,  $d$  and  $N$  previously established. However, these values can be adjusted to fit different lens areas depending on the amount of solar energy required. For example, a Fresnel lens with a larger area requires a greater number of micro-heliostats in the array, a greater micro-heliostat thickness to prevent its mechanical deflection,



etc. For this reason, in the subsequent figures, the values of area are expressed in terms of  $m^2$  and percentage. Thus, for a  $1m^2$  lens, a value of  $0.25m^2$  is equal to 25% of its total area. Likewise, this percentage on a  $2.0m^2$  lens is equivalent to  $0.5m^2$ . With this taken into consideration, the shading area can be observed in Fig. 7(a), which varies according to the hour and month. In December and June the minimum and maximum values are presented, varying approximately from 40% of the total lens area in the morning and afternoon to 100% at noon, respectively. This variability is caused by the micro-heliostats' position with respect to the sun. In December, when the sun's path is closer to the horizon, the sun "sees" a larger micro-heliostat area than in June, when the sun's path is farther from it.

#### 4. Effective area of a Fresnel lens

The effective area is the Fresnel lens zone not affected by blocking or shading. The effective area is expressed by the following equation:

$$A_e = A_F - A_s \tag{11}$$

where  $A_F=1.0m^2$ . The effective area of the Fresnel lens is shown in Fig. 7(b). Its value is inversely proportional to the shading area, varying from 60% of the lens area in the morning and afternoon in December to 0% at noon in June, approximately. The configuration and dimensions of the micro-heliostats ( $t$ ,  $w_{mh}$  and  $d$ ) makes it impossible to equal the effective area of the Fresnel lens with its total area. However, to get close to such an objective, the number of micro-heliostats, so far taken as  $N=10$  for a  $1.0m^2$  Fresnel lens, can be varied.

It is evident from Fig. 6 that  $s_{III}$  can be reduced if it is covered by additional micro-heliostats in the array, so the projection of the last micro-heliostat is close to the final edge of the lens. In addition, it must be noted that the greater the  $\epsilon$ -value, the greater the number of micro-heliostats required, which increases the sun's area of projection on the lens. For this reason, an array's tilt of  $49.054^\circ$  is established, a value that represents the upper limit of the  $\epsilon$ -range previously described. The final number of micro-heliostats is calculated by the following expression

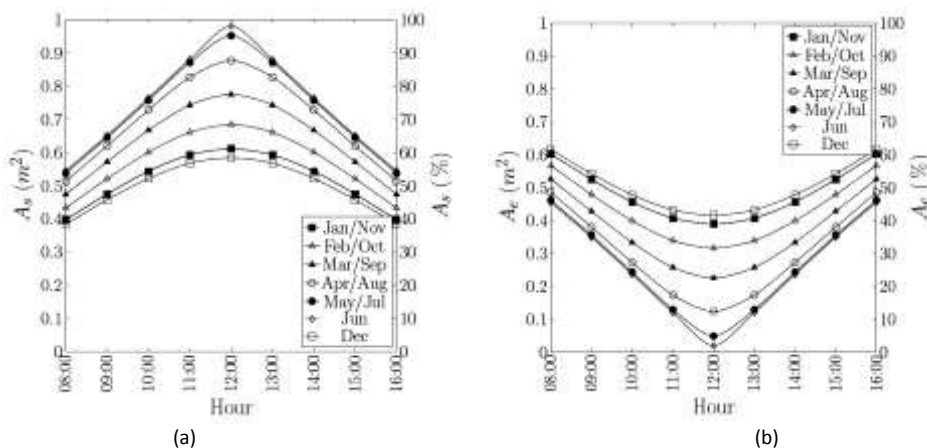


Fig. 7. (a) Shading area on the Fresnel lens throughout the day and year using three values of  $\epsilon$  ( $26.988^\circ$ ,  $38.021^\circ$  and  $49.054^\circ$ ). As the shading area proved to be independent of the array's tilt, only one graphic is shown. (b) Effective area of a  $1.0m^2$  Fresnel lens using  $N=10$ . Area percentage can be seen on the left side of each chart



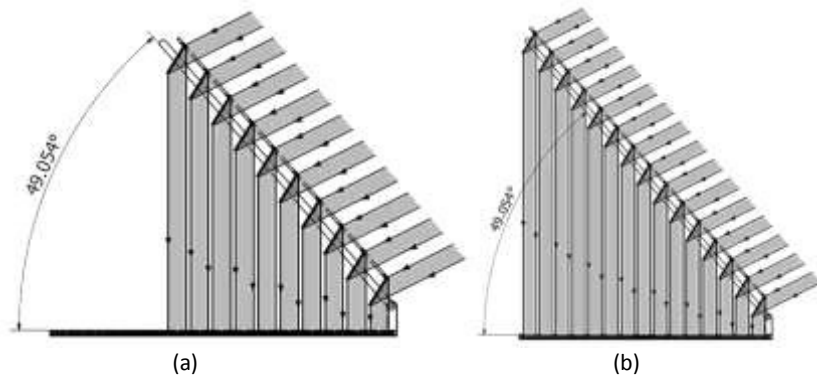


Fig. 8. Comparison between an array with  $N=10$  (a) and  $N_f=15$  (b), both using  $\varepsilon=49.054^\circ$  for a  $1.0\text{m}^2$  Fresnel lens

$$N_f = \text{round down} (w_F / (w_{mh} \cos \varepsilon)) \tag{12}$$

The term *round down* establishes that if the resulting value is not a whole number, it must be rounded down, as it is not possible to have a fraction of a micro-heliostat. Applying equation (12),  $N_f=15$  for a  $1.0\text{m}^2$  Fresnel lens (see Fig. 8). It can be observed that  $s_{III}$  decreases while the effective area increases. The value of the latter is shown in Fig. 9. The effective area varies as a function of the hour and month, from approximately 0% to 90% of the total lens area. Maximum and minimum values are presented in June and December, respectively.

### 5. Conclusions and future work

Solar tracking is a solar concentrator function that raises the complexity and cost of the system. For precise orientation throughout the day and year, a complex electro-mechanical system capable of adapting to latitude changes and environmental conditions is required.

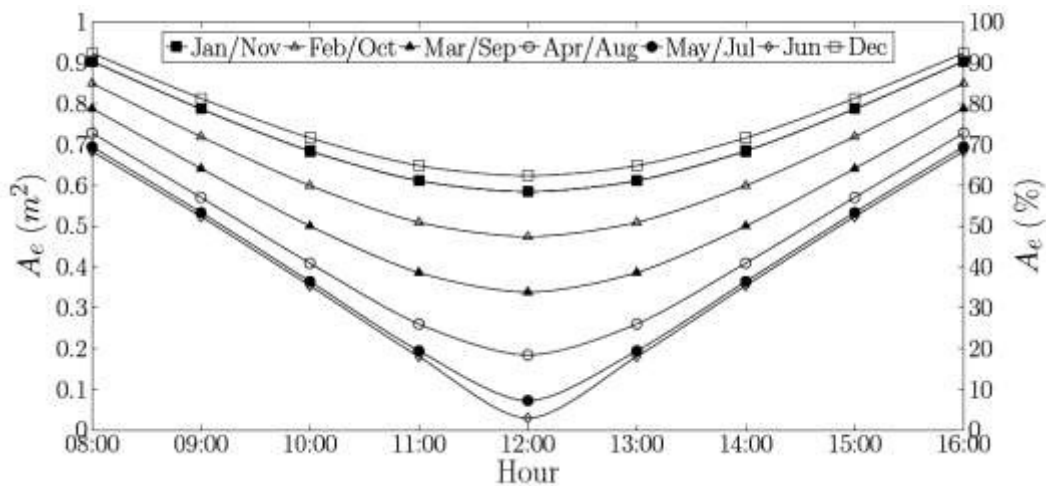


Fig. 9. Effective area of Fresnel lens with  $\varepsilon=49.054^\circ$  and  $N_f=15$

In this research, a solar concentrator system that tracks the sun's position with a minimal mechanical effort and reduced movement was proposed. It mainly consists of a micro-heliostat array, a Fresnel lens and a receiver. The array tracks the position of the sun on two axes: altitude and azimuth. The altitudinal angle is tracked by rotating the micro-heliostats around the  $u$ -axis from  $0^\circ$  to  $40^\circ$  approximately. Likewise, the azimuthal angle is tracked by rotating them around the  $z$ -axis from  $-100^\circ$  to  $100^\circ$  approximately, both from 8:00 to 16:00 hrs on a  $25^\circ 39' 15''$  N latitude. The Fresnel lens is placed underneath the micro-heliostat array and its position remains horizontal, so the wind loads over the whole system are reduced. Finally, there is a receiver placed on the lens focus. Its stationary position releases its weight from the mechanical tracking system, reducing the structural complexity and the amount of energy required for movement.

The array's position above the Fresnel lens causes a reduction of the collection area due to blocking and shading. To reduce both factors, an array's tilt of  $49.064^\circ$  was proposed. This raises the effective area of the Fresnel lens, changing from approximately 0% to 70% of the total lens area in June, and from 70% to 90% in December. These are the maximum values reached by the system for the effective lens area. However, it is evident that only the rays reflected by the micro-heliostats toward the cross-sectional lens area at  $90^\circ$  were considered. There is a Fresnel lens area where the rays passing through the micro-heliostats strike at a different angle. The analysis of these rays will be addressed in future research in an effort to increase the effective area of the lens. Likewise, the values of  $t$ ,  $wmh$ ,  $d$  and  $N$  will be explored to increase the micro-heliostats' mechanical resistance, as well as to reduce the weight to facilitate the tracking of the sun.

### Acknowledgements

To the research group "Solar Thermal Vehicle (STEV)" for support in the development of this project.

### References

- [1] Barone S, Directed Fresnel lenses. 2005, US Patent 2005/0041307A1.
- [2] Johnson K. Fresnel scroll solar tracking Device. 1988, US Patent 4,765,726.
- [3] Baker, J. Multielement optical panel. 1984, US Patent 4,456,783.
- [4] Barone S. Self tracking, wide angle, solar concentrators. 2004, US Patent 6,700,055B2.
- [5] Larbi A. "A new design of a (3D) Fresnel collector with fixed mirrors and tracking absorber", *J Sol Energy Eng* 2000;**122**:63-8.
- [6] Nilsson J, Leutz R, Karlsson B. "Micro-structured reflector surfaces for a stationary asymmetric parabolic solar concentrator", *J Sol Energy Materials & Solar Cells* 2007;**91**:525-33.
- [7] Kribus A, Ries H. "Limonaed: a limited motion, non-shading, asymmetric, ecliptic-tracking dish", *J Sol Energy* 2002;**73**:337-44.
- [8] Gorthala R. Method and apparatus for a passive solar day lighting system. 2001, US Patent 6,299,317B1.
- [9] Curchod D. Solar electric conversion unit and system. 1993, US Patent 5,255,666.
- [10] Dutson D, Haddock J, Kokonaski W, Blum R, Colbert D. Method for light ray steering. 2007, US Patent 2007/0157924A1.
- [11] Pender J. Motion-free tracking solar concentrator. 2005, US Patent 6,958,868.
- [12] Duffie J, William A. *Solar engineering of thermal processes*. 2nd ed. New York: John Wiley & Sons, Inc.; 1991.
- [13] Leutz R, Suzuki A. *Nonimaging Fresnel lenses: design and performance of solar concentrators*. New York: Springer; 2001.
- [14] Schramek P, Mills D. "Multi-tower solar array", *J Sol Energy* 2003;**75**:249-60.